

New Developments in Processing and Control of Selected Area Laser Deposition of Carbon

W. Richards Thissell and H. L. Marcus

*Center for Materials Science and Engineering
The University of Texas at Austin
Austin TX 78712*

Selected area laser deposition (SALD) has been used to deposit carbon from methane, hydrogen, oxygen, and argon mixtures using a third generation deposition system. The effect of two laser scanning hardware/software designs on the development of morphological instability in the resulting deposit is compared. One method uses programmed I/O using the main process control CPU to calculate and download beam position and desired laser power. Another method is presented which uses dedicated direct memory access (DMA) controllers and a dedicated counter/timer to download the required information. Its improvements to the process include better coordination between laser power and beam speed resulting in an improved beam power delivery uniformity and an improved ability to utilize one CPU for control of more of the SALD process variables.

1. INTRODUCTION

A process being developed at The University of Texas at Austin is solid freeform fabrication (SFF)^{1,2} using selected area laser deposition (SALD).^{3,4,5} The overall goal of this project is to make arbitrary three dimensional parts from solids deposited out of the vapor phase without human intervention or part specific tooling. The geometry and desired material are defined by a solid modeling computer file. SALD is a mechanism developed here at the University to accomplish this. SALD is accomplished by directing a laser beam normal to a surface and to move this beam relative to the surface. The surface is locally heated where the laser beam impinges upon it. Chemical vapor deposition (CVD) or laser ablation can occur when the surface is at certain temperatures. The physics of the process are extremely complicated. For example, SALD involves the formation of three-dimensional hemispherical boundary layers around the moving deposition regime^{6,7} and the substrate heating is a transient, moving boundary value problem.^{8,9,10,11,12} Intense photon flux and thermal energy at the substrate surface is known to create plasmas under certain conditions via either a multiphoton induced ionization mechanism or by direct interaction by electrons with the strong electromagnetic fields that exist in focused laser beams via inverse bremsstrahlung, leading to a cascade mechanism.¹³

SALD can be used to achieve very high rates of deposition, when measured in units of length/time. This can be partially explained by the formation of a three-dimensional boundary layer, while a one-dimensional boundary layer exists for large area CVD processes. This three dimensional boundary layer results in much larger fluxes of reactants to the deposition surface and products away from the deposition surface. Carbon rod growth rates of up to 1 mm/s have been measured from 99.6% pure acetylene.⁴ SALD deposition rates of this order are desirable for making SFF of structural parts a viable process. However, high deposition rates from SALD may not be required for commercial success using SALD for SFF because SALD can be used to make materials for which there is no current manufacturing process. For example, SALD has the potential to be employed to make arbitrary three dimensional parts out of diamond and diamondlike carbon (henceforth, both diamond and diamondlike carbon will be called *sp*³ bonded

carbon). This would allow virtually unlimited applications to employ sp^3 bonded carbon's unexcelled hardness, isotropic modulus, chemical inertness, thermal conductivity, and tribological properties.

This paper documents the current state of the process machine. Preliminary deposition studies are then described. The development of morphological instability as the result of inadequate coordination between laser power control and beam scan velocity is illustrated. An improved controller computer interface and software design results in a great improvement in deposit uniformity and morphological stability.

2. SALD Machine Description

The design of the SALD machine described herein has been described previously in the literature.¹⁴ The process machine is a third generation SALD machine and is the first attempt at computer integration of most of the significant process variables. The design goal of the process machine is to bring the significant process parameters under sufficient control such that SALD may be developed into a viable process for depositing arbitrary three dimensional parts directly from the gas phase from solid model data. Concurrent engineering principles have been utilized in developing the process machine and the process. A schematic overview of the major machine elements is shown in figure 1. A brief description of the laser scanning sub-system follows.

The process laser is a Synrad Duolase 50 and is a 50 W circularly polarized CO_2 laser. A visible HeNe laser (5 mW, 632 nm) is combined with the process beam immediately at its exit to facilitate optical alignment. The combined beams are then immediately expanded by a ten times Galilean beam expander and are then focused about 0.5 m from the exit aperture of the laser by a plano-convex lens of 0.5 m focal length. The beam profile at the focal lens has a profile approximately halfway between the rectangular profile of the beam at the exit aperture of the laser and a fully developed Gaussian profile. The beam is then steered into the process chamber by the galvanometers. Its profile is substantially Gaussian at the beam waist and has a $1/e^2$ diameter of about 250 μm , yielding a composite optical system $M^2 = 1.10$, meaning that the real beam waist is about ten percent larger than the theoretically minimum beam waist.

The laser power is controlled in real time by a combination of a direct memory access (DMA) controlled 12 bit D/A converter and a custom designed electronic circuit that translates the computer controlled analog signal into a 20 kHz pulse width modulated laser control signal. This configuration allows for precise (within the specified ± 5 percent output power fluctuation intrinsic to the laser) laser power control that can be coordinated in real time with the galvanometer based scanning setup.

The laser scanning is accomplished with Cambridge Technologies, Inc. 6650 galvanometers and a dedicated analog PID controller from the same manufacturer. The advantage of this scanning system compared to strictly vector based scanning systems is that this system can scan arbitrary curves in the process plane without approximating the curve by a series of vectors where the beam is started and stopped at the corresponding vector line endpoints.¹⁵ Starting and stopping the laser beam movement over the process surface results in uneven power delivery that is difficult to control. Precise beam steering on the process plane at constant velocity is achieved by changing the setpoint in angular position sent to the controller in real time. The desired process plane beam position is readily converted to a mirror angular position exactly by a simple trigonometric expression without the need of a complex calibration procedure or look-up table corrections. The most difficult aspect of the scanning control is calculating and

downloading these points to the controller in real time and coordinating this procedure with real time laser power control.

A first attempt involved a simple digital I/O board that utilized an Intel 8255 controller that is the heart of the floppy drive interface used in industry standard computers. This controller required a programmed I/O under the mode required to interface with the analog PID controller. Both repeatable and random deposition irregularities during the process experimentation indicated that this method was too casual with respect to time for the needs of the SALD process. It also had severe implications on the development of integrated control of other process variables. The scanning algorithm caused a software timer to expire every 250 μ s that would result in the main program's event loop to execute a function that calculates and downloads new positions based on

SALD System III Schematic Overview

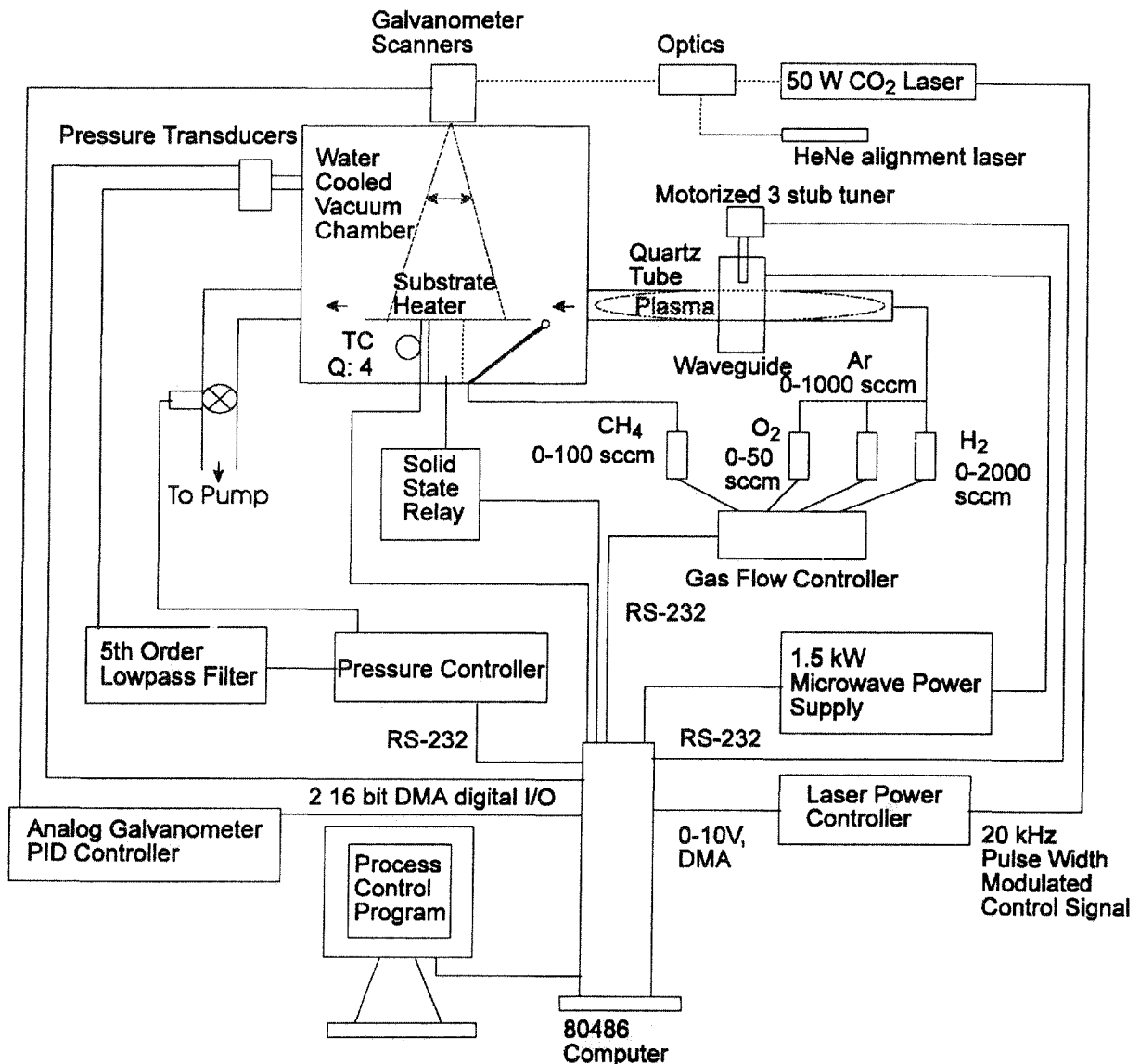


Figure 1: Schematic overview of the third generation SALD process machine. The two major elements of focus of this schematic are the process vacuum chamber and the computer. Control lines fan to and from the computer to various dedicated process controllers, electronic circuits, and modules. Likewise, gases, microwave, laser, and electric heater power flow to the reactor, and sensor information flows from the reactor.

the current time. The stringent real time requirements of the laser beam scanning control precluded other process control modules or GUI operator requests from being executed whilst the beam was on and being scanned. Furthermore, periodic interrupts occur in the process program that can take up to one to two milliseconds to execute which effectively causes the galvanometer mirrors to slow down or stop when these interrupts occur during beam scanning. A practical consequence of the presence of the interrupts is that the DMA laser power array cannot be synchronized with the true end of the scan curve, preventing the utilization of a power ramp down at the end of the scan line. The origins of these interrupts are intrinsic to DOS and the memory managers required to execute the 16 bit protected mode process control program running on an industry standard architecture 33 Mhz Intel 804086 computer with 256 kB of 15 ns cache and 16 MB of 60 ns DRAM. The original programmed I/O configuration turned off the laser when the analog PID control sent a settling signal indicating that the mirrors are within 0.05 degrees mechanical ($\sim 5 \times 10^{-4}$ m on the scan plane) of the setpoint.

A solution to this power delivery problem was engineered by changing the computer interface board to a 32 bit digital I/O board that utilizes two 16 bit DMA channels and a dedicated timer/counter to coordinate data transfers to the analog PID controller. The beam position data transfers are synchronized with the laser power data transfers. The circuitry of the analog controller also had to be modified so that it would accept the data transfer protocol used by the new I/O board. The analog PID controller was further modified so that the settling signal is sent when the mirrors are within 0.0025 degrees mechanical ($\sim 2.5 \times 10^{-5}$ m). The main process control CPU is removed from the stringent real time requirements in the new method, greatly facilitating improved overall process control and user response. The CPU calculates arrays of data for each scan line or arbitrary curve for each mirror axis and the laser power, and three 16 bit DMA channels and a counter/timer handle the transfer of these arrays from system memory across the I/O bus to the process control boards.

Although the new scanning computer interface and software design resulted in much improved laser power delivery uniformity, it is not optimized with our present computer capability. Optimizing the DMA laser scanning software will involve building a 32 bit protected mode program that will decrease the magnitude of the array calculation imposed delays by a factor of two and switching the CPU to a readily available 90 or 100 Mhz Pentium™ processor will approximately decrease the calculation imposed delay by another factor of ten or more. Another optimization will involve changing from the current single DMA buffer for each channel to a dual buffer configuration.

The integration of the SALD machine with solid model data files is a major ongoing goal of the SALD development process. The current state of this development takes industry standard ".STL" files and slices and dices them with two command line filters developed here at the University in a cooperative effort by several researchers. The versions of these programs used for the SALD process development are 32 bit protected mode, virtual memory versions running on top of DOS, Windows, or OS/2. The data file that the second of the filters emits contains laser scan data that can include contours and x and/or y axis laser scan lines for each of the solid model slices. The current contour description implementation is a series of straight line segments due to the intrinsic nature of faceted ".STL" files. The data coordinates represent coordinates on a scan plane as unsigned integers. The process control program takes these data files as input and exactly translates these coordinates to corresponding mirror angular positions. The process

control program is currently implemented as a 16 bit protected mode program using virtual memory and a graphical user interface running under DOS.

3. Deposition Experiments

Silicon wafers were used as substrate materials. Silicon has near zero transmittance at 10.6 μm radiation at temperatures above 400 $^{\circ}\text{C}$ and a normal spectral reflectance of about 0.2-0.25 when doped with impurities less than $2 \times 10^{19} \text{ cm}^{-3}$ which rises to about 0.7 when doped with impurities of about $7 \times 10^{19} \text{ cm}^{-3}$.¹⁶ Graphite has a normal spectral reflectance of about 0.61 at 25 $^{\circ}\text{C}$ and at 10.6 μm radiation and an estimated normal spectral transmittance of about 0.9 under the same conditions, based on trends indicated by data taken at 8 to 9 μm .¹⁷

Figure 2 shows a cross section of the scanned data file which represents a gear. The laser scanned pattern first traces the contour of the gear and then performs both a x and a y axis vector fill all at a given laser power and scan speed with a beam spacing of $1.0 \times 10^{-4} \text{ m}$ for each layer. A series of gears were scanned over the wafer, usually under different combinations of scan velocity and laser power holding other parameters constant. A typical grouping of spacings used is shown in figure 3.

Morphological instability refers to increasing topological roughness as growth rates and deposit thickness increase.^{18,19,20,21} Several tests were also made to determine the magnitude of the development of morphological instability as the number of scan layers is increased. These tests were initially performed using the initial programmed I/O laser scanning

Dimensions are in SI (meters)

Figure 2: Cross section of a solid model of a the gear used in the heated Si wafer SALD experiments.

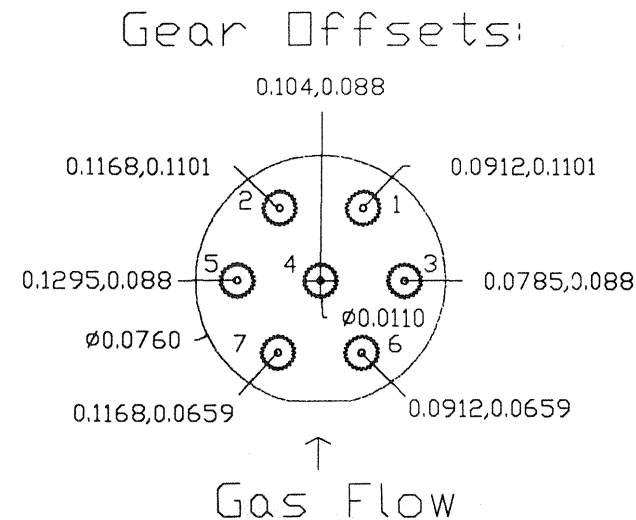
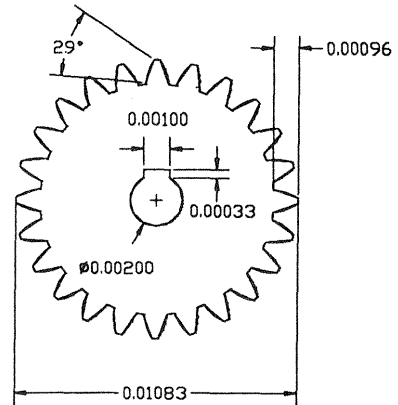


Figure 3: Typical arrangement of gear laser scan patterns on silicon substrate. The listed coordinates are offsets entered into the process control program and are in meters.

arrangement and demonstrated its inadequacy at controlling morphological instability. The silicon wafer experiments were performed with a substrate bias temperature ranging from 400-800 $^{\circ}\text{C}$ and differing methane and hydrogen flow rates that result in a mole fraction of methane ranging from 1.5 to 14 percent methane in hydrogen, pressures ranging from 66 Pa to 50 kPa (0.5-375 Torr), and several different laser powers, P_l , and scan speeds, v_l , that covered about two orders of magnitude of laser fluence, F_l . The laser power up ramp time is τ_r and the laser power down ramp time is τ_e where negative values indicate a laser power ramp completes when the end of the scan curve is reached and positive values mean the ramp down begins after the the end of the scan curve is reached.

Figure 4 is an SEM of an outer surface of a cylindrical deposit that was used prior to the development of the gear model. It illustrates the random and systematic variations in deposition rate that are attributed to the programmed I/O laser scanning configuration.

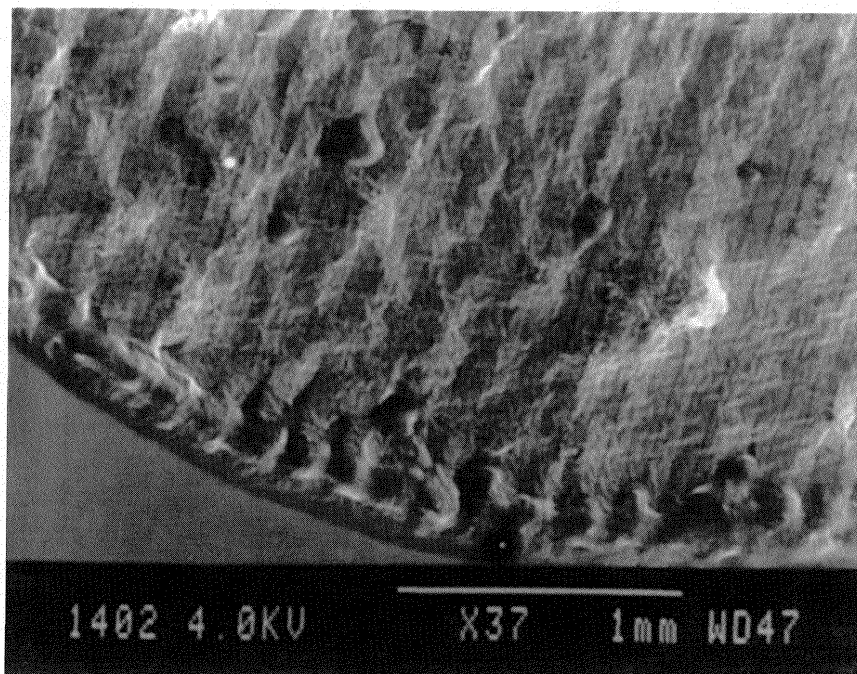


Figure 4: SEM of a laser scanned cylinder, illustrating the random and systematic variation in deposition height resulting from the initial programmed I/O laser scanning configuration. $T_s = 700\text{ }^\circ\text{C}$, 14 sccm CH_4 , 100 sccm H_2 , 50 kPa (375 Torr), $v_f = 0.01\text{ m/s}$, 25 layers, $P_f = 40\text{ W}$ ($F_f = 2.2 \times 10^7\text{ Ws/m}^2$), $\tau_s = 200\text{ }\mu\text{s}$, $\tau_r = 0\text{ }\mu\text{s}$.

Figure 5 is an SEM of a typical SALD gear and shows the variation of deposit thickness that is characteristic of the laser scan pattern. Note the bumps on the beginning and end of each scan line. Figure shows a center of a SALD gear where a nearly vertical contour deposit edge occurs with cone shaped deposits. The vertical wall is about $100\text{ }\mu\text{m}$ high. This systematic deposition irregularity, combined with random deposition irregularities which partially result from the effect of computer interrupts, accumulate as the number of scan layers increases and can result in a process instability.

A dramatic climax to the development of this instability occurred during of the morphological instability study. Six gears were scanned with increasing number of scan layers from 25 to 300 under otherwise identical conditions. Five of the gears with 25-150 scan layers appear substantially similar, but the deposition rate of the sixth gear started to take off after about 190 layers, preferentially on the scan line end points and on rod like deposits randomly dispersed over the gear surface. Homogeneous gas phase nucleation took over and a sooty deposit formed. The rod like deposits that surrounded the contours of the gear grew to a height of about 1 cm in about 1-2 hours. The laser coupling into deposit improved sufficiently to result in the melting through of the wafer.

The DMA laser scanning configuration eliminated both the systematic and random variation of deposit thickness across the scanned gear. No morphological indication of the scan

pattern could be observed by SEM, as is shown in figure 6 in the deposited region of the gear. An example of the smoothness of the ends of the scan curve is shown in figure 7. This SEM also shows some webbing between scan lines that occurs due to the power decay associated with the time constant of the laser ($\tau_l = 150 \mu\text{s}$). The lasing decay results in deposition as the beam is steered from the end of one scan line to the beginning of the next. The laser power during this rapid beam steering is a function of its power during the curve scan, the absolute magnitude of τ_e , and the dwell time provided after each scan line before moving the beam to the beginning of the next. This webbing occurred in both the programmed I/O and DMA laser scanning configurations. The decrease in the beam settling window size made as part of the analog PID controller modifications for implementation of the DMA method facilitated a variable dwell time at each contour end point. The magnitude of this dwell time was increased until the webbing disappeared. Figure 8, to be compared with figure 7, shows a couple of gear teeth where the webbing is almost completely eliminated.

Additional SALD process efficiency will occur when the laser spends a higher fraction of real time lasing. The new DMA scanning method currently calculates the scan and laser power arrays between every scan curve when the laser is not lasing. This time may be significantly decreased by increasing the speed of the processor and changing from 16 bit to 32 bit protected mode operation. Process efficiency may also be improved using a double buffer configuration where one set of arrays are calculated while another set is used to perform a scan. The laser dwell time spent at a laser scan curve endpoint before moving to the beginning of the next curve also

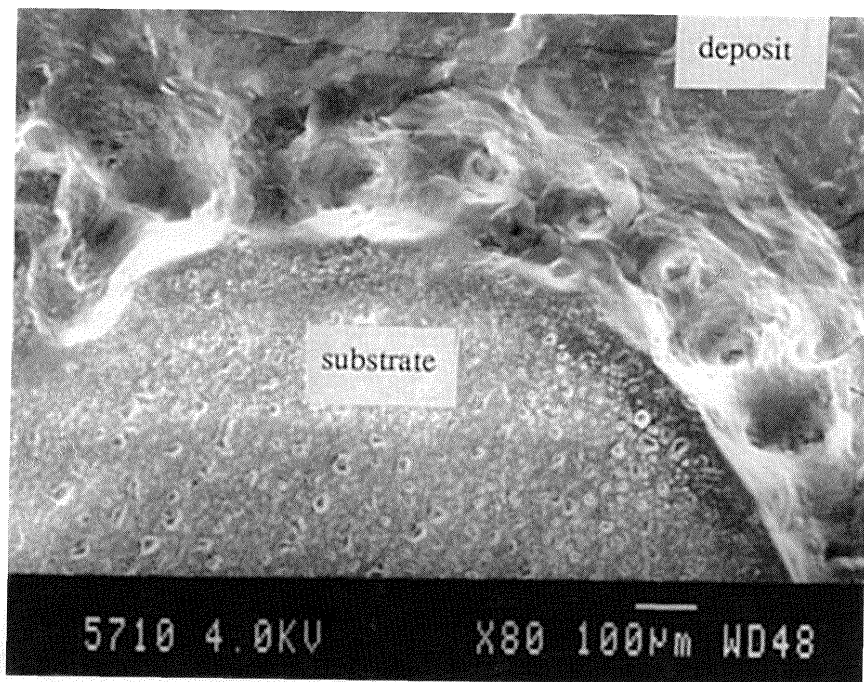


Figure 5: SEM of a laser scanned gear at the gear hole, illustrating the systematic variation in deposition height that results from the initial programmed I/O laser scanning configuration. The deposit rods are nearly vertical and extend about $100 \mu\text{m}$ above the substrate. $T_s = 800 \text{ }^\circ\text{C}$, 42 sccm CH_4 , 300 sccm H_2 , 10 kPa (75 Torr), $v_l = 0.025 \text{ m/s}$, 63 layers, $P_l = 40 \text{ W}$ ($F_l = 1.2 \times 10^7 \text{ Ws/m}^2$), $\tau_s = 200 \mu\text{s}$, $\tau_e = 0 \mu\text{s}$.

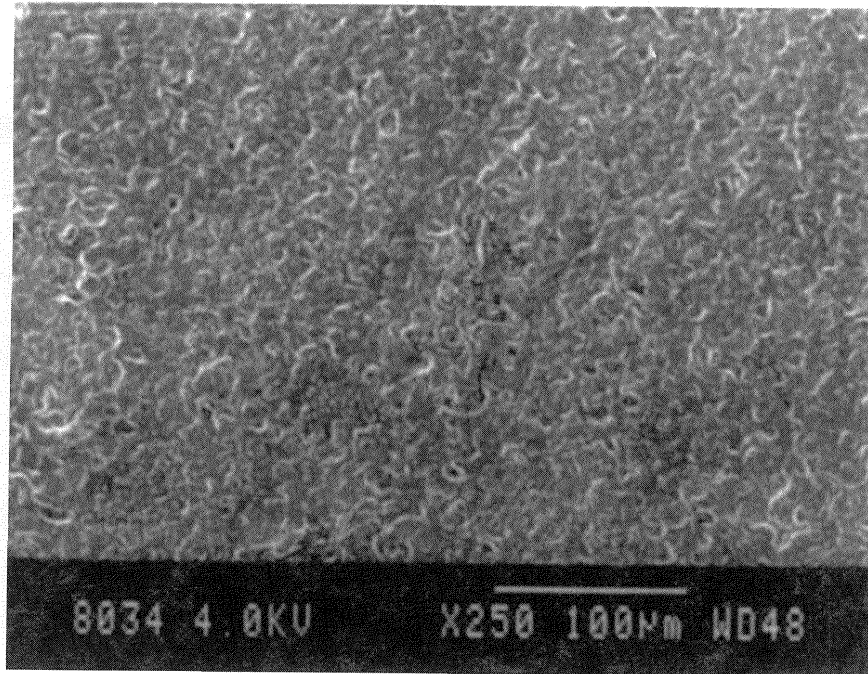


Figure 6: SEM of a laser scanned gear using the DMA laser scanning configuration. No visible indication can be observed by SEM to indicate the laser scanning pattern when this method is properly implemented. $T_s = 700\text{ }^\circ\text{C}$, 9 sccm CH_4 , 300 sccm H_2 , 50 kPa (375 Torr), $v_r = 0.025\text{ m/s}$, $P_l = 20\text{ W}$ ($F_l = 3 \times 10^6\text{ Ws/m}^2$), 600 scan layers, $\tau_s = 2000\text{ }\mu\text{s}$, $\tau_d = -1000\text{ }\mu\text{s}$.

decreases SALD process efficiency. This dwell time may be decreased at the cost of at least fifty percent of the laser power by a photo-acoustical modulator. Alternatively, a high speed shutter may be used to decrease the dwell time without the cost of laser power intrinsic to photo-acoustical modulators.

4. Conclusions

SALD has been used to deposit carbon from methane and hydrogen mixtures using a third generation deposition system. Initial systematic and random morphological instabilities develop as the deposit grows thicker are attributed inadequate laser scan control in the initial programmed I/O scanning configuration. A new DMA based laser scan configuration was designed, prototyped, tested and refined until the systematic and random morphological deposit growth instabilities ceased. This scanning method integrates contour scanning with both x and y axis scanning for each part layer with real time laser power control. This method is applicable to other laser material processes besides SALD.

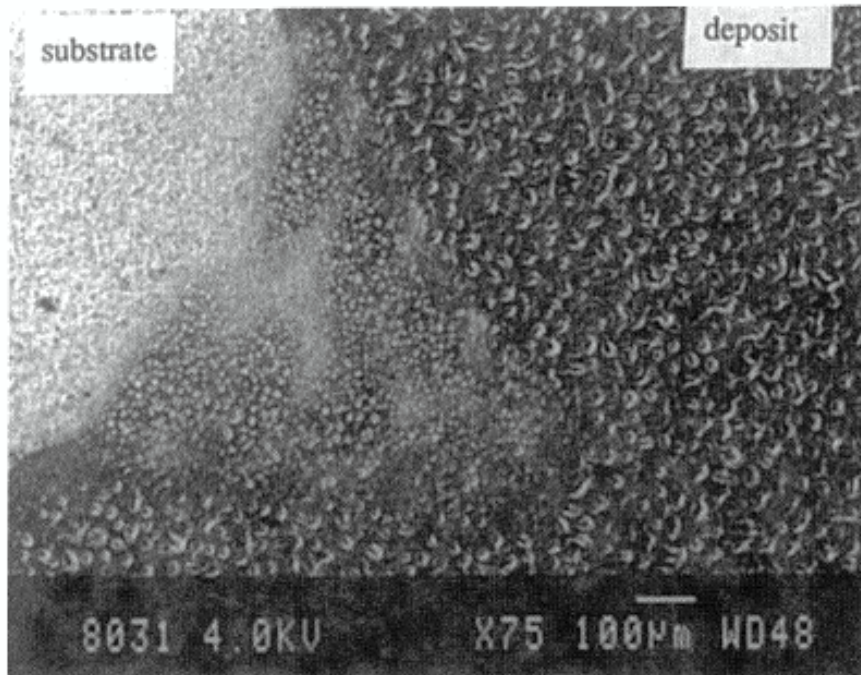


Figure 7: SEM of a laser scanned gear using the DMA laser scanning configuration. $T_s = 700\text{ }^\circ\text{C}$, 9 sccm CH_4 , 300 sccm H_2 , 10 kPa (75 Torr), $v_f = 0.025\text{ m/s}$, $P_l = 20\text{ W}$ ($F_l = 3 \times 10^6\text{ Ws/m}^2$), 50 scan layers, $\tau_s = 2000\text{ }\mu\text{s}$, $\tau_e = -1000\text{ }\mu\text{s}$.

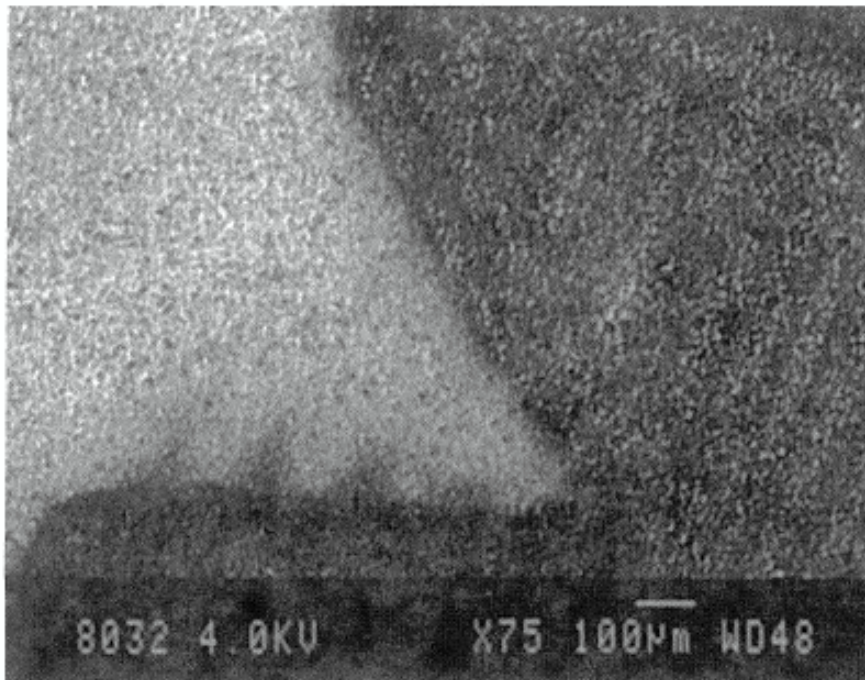


Figure 8: SEM of a laser scanned gear using the DMA laser scanning configuration. $T_s = 700\text{ }^\circ\text{C}$, 9 sccm CH_4 , 300 sccm H_2 , 50 kPa (375 Torr), $v_f = 0.025\text{ m/s}$, $P_l = 20\text{ W}$ ($F_l = 3 \times 10^6\text{ Ws/m}^2$), 50 scan layers, $\tau_s = 2000\text{ }\mu\text{s}$, $\tau_e = -1000\text{ }\mu\text{s}$.

5. Acknowledgments

The authors would like to extend their gratitude to Neal Vail and Suman Das whose tutelage in C and assembly languages and sample code greatly facilitated the software development. John Spurgeon of the Mechanical Engineering Electronics Shop provided valuable insight in electronic trouble shooting. This project was sponsored by ONR under contract number: N00014-92-J-1514.

¹Marcus, Harris L., Joseph J. Beaman, Joel W. Barlow, and David L. Bourell, "From Computer To Component In 15 Minutes: The Integrated Manufacture of Three-Dimensional Objects," Journal of Metals, April 1990, 8-10.

²Marcus, Harris L., Joseph J. Beaman, Joel W. Barlow, and David L. Bourell, "Solid Freeform Fabrication: Powder Processing," Ceramic Bulletin, 69, 6, 1990, 1030-31.

³Zong, Guisheng, Robert Cames, Harovel G. Wheat, and Harris L. Marcus, "Solid Freeform Fabrication by Selective Area Laser Deposition," Proceedings of The Solid Freeform Fabrication Symposium, edited by J. J. Beaman, H. L. Marcus, D. L. Bourell, and J. W. Barlow, The University of Texas at Austin, Austin Texas, August 6-8, 1990.

⁴Zong, Guisheng, Yves Jacquot, W. Richards Thissell, and H. L. Marcus, "Solid Freeform Fabrication Using Selective Area Laser Deposition," Plasma and Laser Processing of Materials, edited by Upadhyay, Kamleshwar, TMS, 1991, 23-48.

⁵Thissell, W. Richards, Guisheng Zong, James Tompkins, Britton R. Birmingham, and Harris L. Marcus, "Selective Area Laser Deposition - A Method of Solid Freeform Fabrication," The Solid Freeform Fabrication Symposium Proceedings, edited by J. J. Beaman, H. L. Marcus, D. L. Bourell, J. W. Barlow, and Richards H. Crawford, The University of Texas at Austin, Austin Texas, August 12-14, 1991.

⁶Copley, Stephen M., "Mass Transport During Laser Chemical Vapor Deposition," Journal of Applied Physics, 64, 4, August 15, 1988, 2064-8.

⁷Skouby, D. C. and K. F. Jensen, "Modeling of Pyrolytic Laser-Assisted Chemical Vapor Deposition: Mass Transfer and Kinetic Effects Influencing The Shape of The Deposit," Journal of Applied Physics, 63, 1, January 1, 1988, 198-206.

⁸Burgener, M. L. and R. E. Reedy, "Temperature Distributions Produced In a Two-Layer Structure By a Scanning CW Laser Or Electron Beam," Journal of Applied Physics, 53, 6, June 1982, 4357-63.

⁹Moody, J. E. and R. H. Hendel, "Temperature Profiles Induced By A Scanning CW Laser Beam," Journal of Applied Physics, 53, 6, June 1982, 4364-71.

¹⁰Allen, S. D., J. A. Goldstone, J. P. Stone, and R. Y. Jan, "Transient Nonlinear Laser Heating and Deposition: A Comparison of Theory and Experiment," Journal of Applied Physics, 59, 5, March 1, 1986, 1653-7.

¹¹Kar, A. and J. Mazumder, "Three-Dimensional Transient Thermal Analysis For Laser Chemical Vapor Deposition On Uniformly Moving Finite Slabs," Journal of Applied Physics, 65, 8, April 15, 1989, 2923-34.

¹²Jacquot, Yves, Guisheng Zong, and Harris L. Marcus, "Modeling of Selective Area laser Deposition for Solid Freeform Fabrication," Proceedings of The Solid Freeform Fabrication Symposium, edited by J. B. Beaman, H. L. Marcus, D. L. Bourell, and J. W. Barlow, The University of Texas at Austin, Austin Texas, August 6-8, 1990, 74-82.

¹³Radziemski, Leon J., and David A. Cremers, "Laser-Induced Plasmas and Applications," New York: Marcel Dekker, Inc., 1989.

¹⁴Thissell, W. Richards, James Tompkins, and Harris L. Marcus, "Design of a Solid Freeform Fabrication Diamond Reactor," Proceedings of The Solid Freeform Fabrication Symposium, edited by J. B. Beaman, H. L. Marcus, D. L. Bourell, and J. W. Barlow, The University of Texas at Austin, Austin Texas, August 6-8, 1990, 48-73.

¹⁵Wu, Ying-Jeng Engin, and Joseph J. Beaman, "Laser Tracking Control Implementation for Sff Applications," Proceedings of The Solid Freeform Fabrication Symposium, edited by J. B. Beaman, H. L. Marcus, D. L. Bourell, and J. W. Barlow, The University of Texas at Austin, Austin Texas, August 3-5, 1992, 179-87.

¹⁶Touloukian, Y. S., and D. P. DeWitt, "Thermal Radiative Properties: Metallic Elements and Alloys," in Thermophysical Properties of Matter, Volume 7, Plenum Press, 1972.

¹⁷Touloukian, Y. S., and D. P. DeWitt, "Thermal Radiative Properties: Nonmetallic Solids," in Thermophysical Properties of Matter, Volume 8, Plenum Press, 1972.

¹⁸Ravi, K. V., "Morphological Instabilities In The Low Pressure Synthesis of Diamond," Journal of Materials Research, 7, 2, February 1992, 384-93.

¹⁹C. H. J. Van Den Brekel, and A. K. Jansen, "Morphological Stability Analysis in Chemical Vapour Deposition Processes. I," Journal of Crystal Growth, 43, 1978, 364-70.

²⁰Jansen, A. K., and C. H. J. Van Den Brekel, "Morphological Stability Analysis In Chemical Vapour Deposition Processes. II," Journal of Crystal Growth, 43, 1978, 371-377.

²¹Palmer, Bruce, and Roy G. Gordon, "Local Equilibrium Model of Morphological Instabilities in Chemical Vapor Deposition," Thin Solid Films, 158, 1988, 313-41.